Analyst

PAPER

Colorimetric and ultra-sensitive fluorescence resonance energy transfer determination of H_2O_2 and glucose by multi-functional Au nanoclusters†

Cite this: *Analyst*, 2014, **139**, 1498

Qian Zhao,[a] Shenna Chen,[a] Haowen Huang,*[a] Lingyang Zhang,[a] Linqian Wang,[b] Fengping Liu,[a] Jian Chen,[a] Yunlong Zeng[a] and Paul K. Chu*[c]

Received 9th October 2013
Accepted 5th December 2013

DOI: 10.1039/c3an01906c

www.rsc.org/analyst

Ultra-sensitive colorimetric determination of H_2O_2 is accomplished based on the intrinsic peroxidase-like activity of Au nanoclusters (AuNCs) stabilized by glutathione (GSH). The color change of 3,3,5,5-tetramethylbenzidine (TMB) catalyzed by AuNCs offers an indirect method to measure glucose. This sensing platform makes use of a dual optical signal change, including the color change in an aqueous solution under visible light illumination and an ultra-sensitive fluorescent assay arising from efficient fluorescence resonance energy transfer (FRET) between the AuNCs and oxidized TMB. The detection limits of H_2O_2 and glucose are 4.9×10^{-13} M and 1.0×10^{-11} M, respectively. In addition, enhanced fluorescence is observed from the AuNCs due to the use of ethanol which produces clear changes in the quantum yield and lifetime of the AuNCs. The quantum yield of AuNCs is enhanced from ~12.5% as an isolated fluorophore to 38.9% in an AuNCs–ethanol complex. The enhanced fluorescence lowers the detection limits of H_2O_2 and glucose by 2 orders of magnitude compared to those attained from the original AuNCs.

Introduction

Noble metal nanoclusters comprising several to tens of atoms possess distinct electronic structures and properties that are fundamentally different from those of larger nanoparticles.[1–5] Their unique physicochemical properties have been exploited in molecular electronics,[6] image markers,[7,8] sensors,[9,10] and catalysts.[11,12] In particular, fluorescent Au and Ag nanoclusters have been used in biological imaging,[13,14] ion sensors,[15,16] and biosensors[17] due to their low toxicity, excellent biocompatibility and stability, good solubility, and desirable luminescence properties.

Catalysis is another promising application of noble metal nanoclusters. Gold was initially thought to be catalytically inert, but nano-scale gold has been demonstrated to exhibit excellent catalytic activity in many chemical reactions.[18,19] An important application of Au nanoclusters (AuNCs) is as artificial enzymes.[20,21] Enzyme mimetics receives much interest because natural enzymes have some intrinsic drawbacks. For example, the catalytic activity is sensitive to environmental conditions and the stability is poor due to denaturation.[22,23] Most research activities focus on the fluorescent properties of metal nanoclusters, but their catalytic properties and potential applications in biological or chemical sensing are also quite important. An Au-nanoparticle-based nano-energy-transfer probe has been developed recently for the rapid and ultra-sensitive determination of mercury.[24] The good stability of AuNCs arises from the chemical inertness of the Au core which is completely encapsulated by ligands, thereby rendering their use in fluorescence resonance energy transfer (FRET) possible. As reported in this paper, AuNCs stabilized by GSH are found to possess intrinsic peroxidase-like activity, which catalyzes oxidation of the peroxidase substrate 3,3,5,5-tetramethylbenzidine (TMB) in the presence of H_2O_2, and ultra-sensitive determination of H_2O_2 and glucose is demonstrated.

Experimental

Chemicals

TMB, GSH, $HAuCl_4 \cdot 3H_2O$, 30% H_2O_2, anhydrous ethanol, glucose, glucose oxidase, cupric chloride ($CuCl_2$), ferric chloride ($FeCl_3$), and mercuric chloride ($HgCl_2$) were purchased from Sinopharm Chemical Reagent Co., Ltd. (Shanghai, China). All of the chemicals, unless mentioned otherwise, were of analytical

[a]*Laboratory of Theoretical Chemistry and Molecular Simulation of Ministry of Education, Hunan Provincial University Key Laboratory of QSAR/QSPR, School of Chemistry and Chemical Engineering, Hunan University of Science and Technology, Xiangtan, China. E-mail: hhwn09@163.com; Tel: +86-731-58290045*

[b]*Department of Laboratory, Hunan Provincial Tumor Hospital, The Affiliated Tumor Hospital of Xiangya Medical School of Central South University, Changsha, Hunan Province, China*

[c]*Department of Physics & Materials Science, City University of Hong Kong, Tat Chee Avenue, Kowloon, Hong Kong, China. E-mail: paul.chu@cityu.edu.hk; Fax: +86-852-34420542; Tel: +86-852-34427724*

† Electronic supplementary information (ESI) available. See DOI: 10.1039/c3an01906c

reagent grade and used as received. The aqueous solutions were prepared with doubly distilled water.

Human serum sample processing

All serum samples and red blood cells were obtained from normal volunteers (Hunan Provincial Tumor Hospital, Changsha). The serum samples were stored at 4 °C until use while whole vein blood samples (2 mL each) were separately collected into heparinized containers, diluted using 5 mL phosphate buffer saline (PBS) solution containing 0.9% NaCl, and centrifuged at 2500 rpm for 5 min. After washing three times with PBS, the cells were resuspended in PBS.

All experiments were performed in compliance with the relevant laws and institutional guidelines. Hunan University of Science and Technology and Hunan Provincial Tumor Hospital have approved the experiments.

Synthesis of AuNCs

Freshly prepared aqueous solutions of $HAuCl_4$ (20 mM, 0.50 mL) and GSH (100 mM, 0.15 mL) were mixed with 4.35 mL of distilled water at 25 °C. The reaction mixture was heated to 70 °C under gentle stirring (500 rpm) for 24 h. An aqueous solution of strongly orange-emitting AuNCs was formed. The orange-emitting AuNC solution could be stored at 4 °C for 6 months with negligible changes in the optical properties.

H_2O_2 and glucose detection using AuNCs as a peroxidase mimic

A typical colorimetric analysis for H_2O_2 was performed as follows. Firstly, 50 μL of 5 mM TMB, 50 μL of AuNCs, and 50 μL of H_2O_2 at different concentrations were added to 350 μL of 0.1 M phosphate buffer (pH 6.0). Secondly, the solution was incubated at 30 °C in a water bath for 15 min and the solution was further used in the absorption experiments.

Glucose detection was conducted as follows. 50 μL of 100 ng mL^{-1} glucose oxidase (GOx) and 50 μL of glucose at different concentrations in 0.1 M phosphate buffer (pH 6.0) were incubated at 37 °C in a water bath for 25 min. 50 μL of 5 mM TMB, 50 μL of AuNCs, and 300 μL of 0.1 M phosphate buffer (pH 6.0) were added to the solution and the final mixture was further incubated at 30 °C for 15 min before conducting the absorption measurements.

Characterization of materials

The UV-vis absorption and photoluminescence (PL) spectra were recorded on a Lambda 35 spectrophotometer (PerkinElmer, USA) and F-4500 (Hitachi, Japan) fluorescence spectrometer, respectively. The photoluminescence lifetime was measured by time-correlated single-photon counting (TCSPC) on an Edinburgh Instruments FLSP920 (UK) spectrofluorometer with a pulsed light-emitting diode (LED) as the excitation source. Transmission electron microscopy (TEM) was performed on a Tecnai G2 20 (USA) transmission electron microscope operating at 100 kV.

Results and discussion

Preparation of AuNCs

The AuNCs were prepared according to a previous approach with slight modification.[25] Briefly, aqueous solutions of $HAuCl_4$ and GSH were mixed and allowed to react under gentle stirring at 70 °C for 24 h. The mixture changed from yellow to colorless within minutes and then gradually to light yellow. Fig. 1 depicts the morphology of the Au(0)@Au(I)–thiolate NCs[25] obtained by high-resolution transmission electron microscopy (HR-TEM). The size of the nanoparticles is less than 2 nm and the size distribution is quite narrow. The AuNCs appear light yellow in solution under visible light and there is intense orange luminescence from the solution when irradiated by ultraviolet (UV) light. The UV-vis absorption and fluorescence spectra acquired from the AuNCs are displayed in Fig. 2. When excited by 450 nm light, an emission band at 570 nm is observed and it is indicative of the successful preparation of AuNCs. The AuNCs stored in water at room temperature also show excellent stability.

Catalytic oxidation of TMB by AuNCs

In order to assess the catalytic activity, TMB, which is commonly used to study peroxidase-like activity, was employed.[26–28] Because oxygen dissolved in the solution may oxidize TMB (designated as ox-TMB), dissolved oxygen is removed from all solutions by purging with high purity nitrogen for 10 min. The AuNCs catalyze the oxidation of TMB to ox-TMB by H_2O_2, producing a blue color and a maximum absorbance at 652 nm originating from the ox-TMB, as shown in Fig. 3. The different absorption intensity reflects the different amounts of ox-TMB resulting from the reaction between TMB and H_2O_2 in the presence of AuNCs. Control experiments using TMB in the absence of AuNCs or H_2O_2 show negligible color variation, suggesting that both components are required for the reactions. The results indicate that the AuNCs behave like peroxidase. Since the AuNCs are purified by dialysis to remove unreacted Au(III) before use, the catalytic effect arises from the AuNCs only with no free metal ions in the solution. It has been reported that Au(0) and Au(I) both exist in the AuNCs structure.[29,30] H_2O_2 can adsorb on the surface of the AuNCs and the O–O bond in H_2O_2 can be broken into two $OH^{\bullet}$ radicals by Au(I) and/or Au(0) of the AuNCs.

Relative catalytic activity of AuNCs with pH

The catalytic activity of the AuNCs depends on the solution pH. Fig. 4 displays the peroxidase-like activity of AuNCs between the

Fig. 1 TEM image of the luminescent AuNCs.

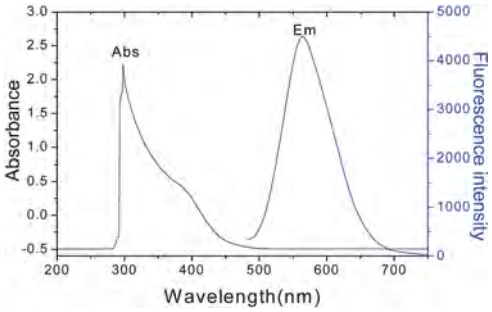

Fig. 2 UV-vis absorption (black line) and photoemission (blue line, $\lambda_{ex} = 450$ nm) spectra of AuNCs.

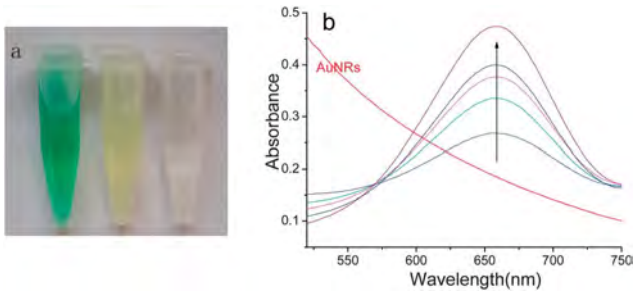

Fig. 3 (a) Photographs of the AuNCs and TMB reaction solution catalytically oxidized by the AuNCs in the presence (left) and absence (middle) of H_2O_2, H_2O_2 and TMB reaction solution in the absence of AuNCs (right). (b) Typical absorption spectra of the TMB solution in the presence of H_2O_2 at various concentrations (from top to bottom: 9.7×10^{-3}, 3.2×10^{-4}, 9.5×10^{-4}, 3.4×10^{-5}, 3.4×10^{-6} M) using AuNCs as an artificial enzyme.

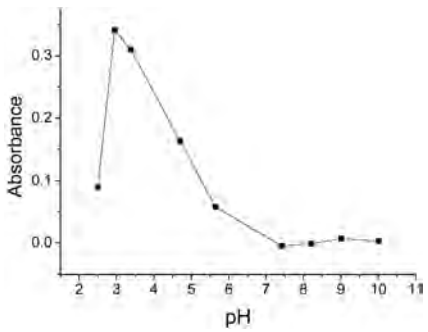

Fig. 4 Relative catalytic activity of AuNCs *versus* pH.

pH values of 2 and 10. The maximum catalytic activity is achieved at a pH of 3.0, and so this pH is used in the subsequent experiments. Hence, catalytic oxidation of TMB with H_2O_2 in the presence of AuNCs is much faster in acidic solutions than in neutral or basic solutions. A possible reason is that the catalytic activity is related to the positive charges of AuNCs.[31] The charge on the GSH is controlled by the pH and the isoelectric point is 5.93.[32] As a result, AuNCs have a greater net positive charge in an acidic solution.

Colorimetric assay for H_2O_2 and glucose

Fig. 3b shows the relationship between the absorbance and H_2O_2 concentration under certain conditions, at which the absorption intensity at 652 nm is proportional to the H_2O_2 concentration. Generally, the color change depends on the amount of ox-TMB produced from TMB in the presence of AuNCs and a visual colorimetric assay for H_2O_2 is possible, as shown in Fig. 5a. Fig. 5b indicates a linear relationship between H_2O_2 concentrations of 1.0×10^{-6} and 1.0×10^{-5} M with a detection limit of 3.2×10^{-8} M.

Since the catalytic activity of AuNCs depends on the H_2O_2 concentration and H_2O_2 is the main product of the glucose oxidase (GOx)-catalyzed reaction, colorimetric determination of glucose can be realized using the AuNCs instead of the traditional horseradish peroxidase. This colorimetric method combined with GOx can be adopted to detect glucose (Fig. 6) in patients suffering from diabetes. To test the efficacy, experiments are performed with human serum. A 20 μL aliquot of serum sample is added to the AuNCs and TMB in the presence of GOx and Fig. S1, ESI† shows the color change.

Similar to natural enzyme catalyzed reactions, the color change depends on the amounts of TMB and H_2O_2, suggesting the amount of glucose can be determined colorimetrically by adjusting the amounts of AuNCs, TMB, and the pH of the solution. The results are shown in Fig. 7. Although the blood glucose level varies at different stages, especially after a meal, if the fasting plasma glucose concentration is greater than 6 mM and the plasma glucose 2 hours after meals is greater than 11 mM, the person is deemed to be clinically diabetic.[33,34] By using this method, the glucose concentration is determined from serum samples from ten healthy volunteers and the results (4.02–7.8 mM) are satisfactory, and most importantly, the technique is largely free from the complicated matrix effect arising from the human serum samples.

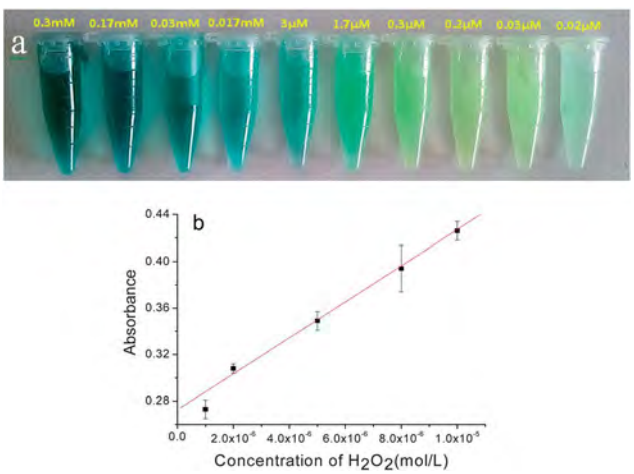

Fig. 5 (a) Photographs showing the color change of AuNCs at various concentrations of H_2O_2 in the presence of TMB under visible light. (b) Linear calibration curve between the absorbance at 652 nm and concentration of H_2O_2, the error bars represent the standard deviation of three measurements.

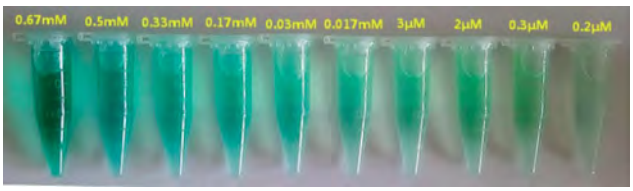

Fig. 6 Photographs showing the color change of AuNCs at various concentrations of glucose in the presence of glucose oxidase, AuNCs, and TMB under visible light.

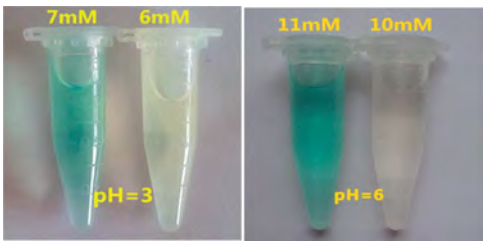

Fig. 7 Photographs showing the colorimetric analysis of different concentrations of glucose by adjusting the pH value.

Fluorescent analysis of H_2O_2 and glucose based on FRET

The AuNCs show fluorescence which does not fluctuate for an hour after the addition of H_2O_2. However, the fluorescent intensity decreases rapidly upon the addition of TMB and further investigation reveals that the fluorescent intensity changes with the concentration of H_2O_2 in the presence of TMB and AuNCs, as shown in Fig. 8. Hence, this sensing system yields a dual optical signal change. Upon addition of TMB to the AuNCs in the presence of H_2O_2, besides the color change under visible light, it is also a useful fluorescent sensor with ultra-sensitivity arising from the efficient FRET between the AuNCs and ox-TMB. Upon oxidation of TMB by H_2O_2 catalyzed by the AuNCs, ox-TMB shows absorption with the maximum at a wavelength of 652 nm. Since the emission spectrum of AuNCs overlaps with the absorption spectrum of ox-TMB, as shown in Fig. 9, there is the possibility of FRET between them. FRET-based analytical methods have advantages including higher sensitivity and simplicity in the detection of ligand–receptor binding by observing the change in the fluorescence from the acceptor.[35,36]

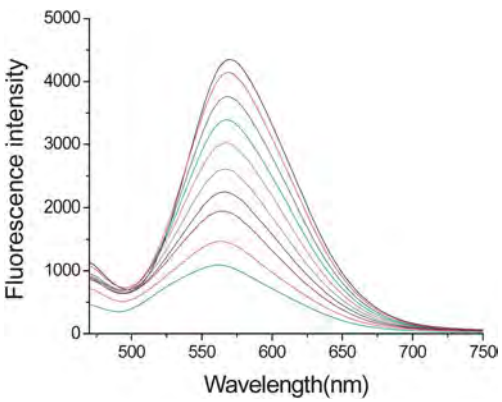

Fig. 8 Fluorescence quenching of AuNCs with increasing H_2O_2 concentration (from top to bottom: 0, 4.9×10^{-13}, 4.8×10^{-12}, 4.7×10^{-11}, 4.5×10^{-10}, 4.4×10^{-9}, 4.3×10^{-8}, 4.3×10^{-7}, 4.2×10^{-6}, 4.1×10^{-5} M) in the presence of TMB.

Steady-state fluorescence measurements are carried out to corroborate energy transfer between the AuNCs and ox-TMB. Emission from AuNCs is drastically quenched in ox-TMB but no fluorescence change is observed when TMB is added to the AuNCs solution. When an ascorbic acid solution is added to the mixture of AuNCs and ox-TMB, the fluorescence intensity gradually increases (Fig. S2, ESI†). Since the reduction reaction between ascorbic acid and ox-TMB converts ox-TMB into TMB, the absorption intensity at 652 nm decreases with the amount of ox-TMB, implying that fluorescence quenching arises from FRET between the AuNCs and ox-TMB.

AuNCs play a dual role in this process, as shown in Scheme 1. Firstly, the AuNCs mimic peroxidase enabling TMB to react with H_2O_2 producing ox-TMB. Secondly, the AuNCs are a FRET donor. The produced ox-TMB is in full contact with the AuNCs in the solution thus meeting the requirement for FRET because the AuNCs and ox-TMB are mixed well and the distance between the two species is less than 10 nm.[37–39] Meanwhile, the ox-TMB serves as an acceptor showing an absorption peak at 652 nm that overlaps with the emission band from the AuNCs excited at 450 nm. If no AuNCs are present, it is impossible to perform the colorimetric assay. Under the appropriate conditions, a larger amount of H_2O_2 generates more ox-TMB and the acceptor shows strong absorption in the AuNCs' emission region. Therefore, spectral overlap increases and the acceptor ox-TMB decreases the fluorescence by FRET. The concentration of H_2O_2 can be determined by measuring the variation in the fluorescence intensity, as shown in Fig. 10 which reveals an ultra-low detection limit for H_2O_2 of 4.9×10^{-13} M. In the absence of H_2O_2, no ox-TMB is produced and there is no spectral overlap between the AuNCs' emission and TMB absorption. Obviously, FRET is suppressed and the fluorescence intensity does not change. From the perspective of sensing applications, this assay can be extended to determine glucose to a detection limit of 1.0×10^{-11} M and good linearity is revealed between 6×10^{-10} and 2×10^{-9} M, as shown in Fig. S3, ESI.†

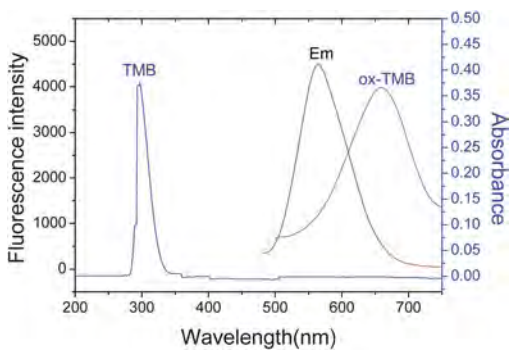

Fig. 9 UV-vis absorption spectra of TMB and ox-TMB and photo-emission (λ_{ex} = 450 nm) spectrum of AuNCs.

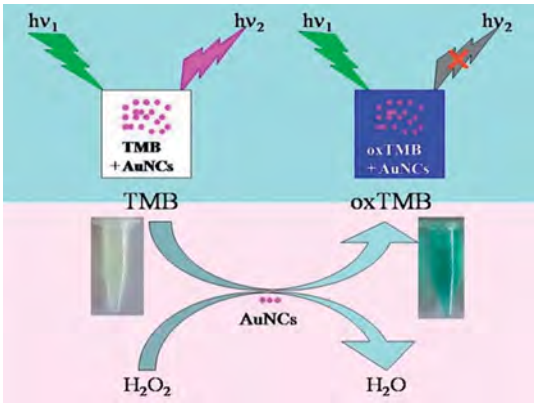

Scheme 1 Schematic illustration of colorimetric and fluorometric detection of H_2O_2 by AuNCs.

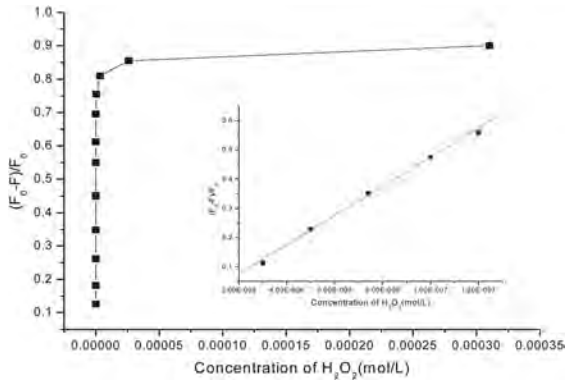

Fig. 10 Concentration-dependent fluorescence intensity of H_2O_2 on the AuNCs in the presence of TMB, where F_0 and F are the fluorescence intensity of the AuNCs at 580 nm in the absence and presence of H_2O_2, respectively. The inset shows a good linear relationship in the concentration range of 2×10^{-8} to 1.3×10^{-7} M with the regression coefficient $R = 0.9985$.

Fluorescence enhancement with ethanol

In this study, the TMB solution is prepared by dissolving solid TMB in ethanol. Interestingly, increased fluorescence is also observed when the TMB ethanol solution is added to the solution of AuNCs. Further investigation indicates that ethanol rather than TMB may enhance fluorescence. The changes in the optical properties induced by ethanol are monitored *in situ* by acquiring fluorescence spectra at various concentrations. Fig. 11 shows the plot of the fluorescence intensity at 570 nm *versus* ethanol concentration and it can be divided into two stages. In the first stage, the intensity increases with ethanol concentration and the largest intensity is observed at a concentration of 75%. At this ethanol concentration, the fluorescence intensity at 570 nm increases by 4.4 times compared to that of the original AuNCs.

Ethanol can also influence the quantum yield and lifetime of the AuNCs, as shown in Fig. S4, ESI.† The quantum yield increases from 12.5% to 38.9% and the lifetime changes from $\tau_1 = 1.3884$ μs (56.44%) and $\tau_2 = 7.809$ μs (43.56%)

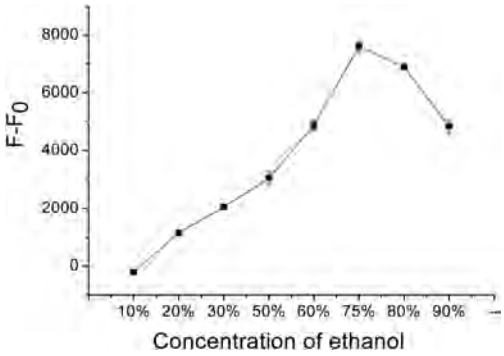

Fig. 11 Fluorescence intensity of AuNCs *versus* concentration of ethanol, where F_0 and F are the fluorescence intensity of the AuNCs at 570 nm in the absence and presence of ethanol, respectively.

to $\tau_1 = 2.9947$ μs (25.28%) and $\tau_2 = 10.672$ μs (74.72%). The application to the detection of H_2O_2 and glucose is illustrated in Fig. S5, ESI† and the detection limit can be reduced by 2 orders of magnitude compared to the original AuNCs.

Conclusions

Colorimetric and ultra-sensitive FRET-based determination of H_2O_2 and glucose by employing multi-functional AuNCs is demonstrated. The AuNCs stabilized by GSH exhibit intrinsic peroxidase-like activity rendering the colorimetric determination of H_2O_2 possible. Monitoring of the color change of TMB catalyzed by AuNCs offers an indirect method to determine the glucose concentration optically. Efficient FRET between the strongly fluorescent AuNCs and ox-TMB yields ultra-low detection limits for H_2O_2 and glucose of 4.9×10^{-13} M and 1.0×10^{-11} M, respectively. The dual optical signal change can be utilized to detect H_2O_2 and glucose colorimetrically and by monitoring the fluorescence. Significant fluorescence enhancement by ethanol is observed and it results in changes in the quantum yield and lifetime of the AuNCs. The quantum yield of the AuNCs is increased from ~12.5% as an isolated fluorophore to 38.9% in the AuNCs–ethanol complex. This technique has tremendous potential in ultra-sensitive determination of H_2O_2 and glucose and the detection limit of H_2O_2 is reduced by two orders of magnitude compared to that accomplished from the original AuNCs.

Acknowledgements

This work was supported by the National Natural Science Foundation of China (21075035, 21375036, 51373002, 51003026), the Innovation Platform Open Funds for Universities in Hunan Province (13K090), and Guangdong–Hong Kong Technology Cooperation Funding Scheme (TCFS) GHP/015/12SZ.

Notes and references

1 Y. Negishi, Y. Takasugi, S. Sato, H. Yao, K. Kimura and T. Tsukuda, *J. Am. Chem. Soc.*, 2004, **126**, 6518.
2 L. Shang, D. Shaojun and G. Nienhaus, *Nano Today*, 2011, **6**, 401.

3 Y.-C. Shiang, C.-C. Huang, W.-Y. Chen, P.-C. Chen and H.-T. Chang, *J. Mater. Chem.*, 2012, **22**, 12972.
4 D. M. Chevrier, A. Chatt and Z. Peng, *J. Nanophotonics*, 2012, **6**, 064504.
5 X. Yuan, Z. Luo, Y. Yu, Q. Yao and J. Xie, *Chem.–Asian J.*, 2013, **8**, 858.
6 C. M. Aikens, *J. Phys. Chem.*, 2011, **2**, 99.
7 C. A. J. Lin, T. Y. Yang, C. H. Lee, S. H. Huang, R. A. Sperling, M. Zanella, J. K. Li, J. L. Shen, H. H. Wang, H. I. Yeh, W. J. Parak and W. H. Chang, *ACS Nano*, 2009, **3**, 395.
8 I. Díez and R. H. A. Ras, *Nanoscale*, 2011, **3**, 1963.
9 B. Adhikari and A. Banerjee, *Chem. Mater.*, 2010, **22**, 4364.
10 N. Goswami, A. Giri, M. S. Bootharaju, P. Lourdu Xavier, T. Pradeep and S. K. Pal, *Anal. Chem.*, 2011, **83**, 9676.
11 L. Hu, Y. Yuan, L. Zhang, J. Zhao, S. Majeed and G. Xu, *Anal. Chim. Acta*, 2013, **762**, 83.
12 X. Nie, H. Qian, Q. Ge, H. Xu and R. Jin, *ACS Nano*, 2012, **6**, 6014.
13 X. Huang, Y. Luo, Z. Li, B. Li, H. Zhang, L. Li, I. Majeed, P. Zou and B. Tan, *J. Phys. Chem. C*, 2011, **115**, 16753.
14 L. L. Ma, J. O. Tam, B. W. Willsey, D. Rigdon, R. Ramesh, K. Sokolov and K. P. Johnston, *Langmuir*, 2011, **27**, 7681.
15 J. L. MacLean, K. Morishita and J. Liu, *Biosens. Bioelectron.*, 2013, **48**, 82.
16 J. Xie, Y. Zheng and J. Y. Ying, *Chem. Commun.*, 2010, **46**, 961.
17 X. X. Wang, Q. Wu, Z. Shan and Q. M. Huang, *Biosens. Bioelectron.*, 2011, **26**, 3614.
18 D. Tang and C. Hu, *J. Phys. Chem. Lett.*, 2011, **2**, 2972.
19 H. Qian, D. Jiang and G. Li, *J. Am. Chem. Soc.*, 2012, **134**, 16159.
20 Y. Tao, Y. Lin, Z. Huang, J. Ren and X. Qu, *Adv. Mater.*, 2013, **25**, 2594.
21 F. Wen, Y. Dong, L. Feng, S. Wang, S. Zhang and X. Zhang, *Anal. Chem.*, 2011, **83**, 1193.
22 W. He, Y. Liu, J. Yuan, J. J. Yin, X. Wu, X. Hu, K. Zhang, J. Liu, C. Chen, Y. Ji and Y. Guo, *Biomaterials*, 2011, **32**, 1139.
23 J. Wang, D. Han, X. Wang, B. Qi and M. Zhao, *Biosens. Bioelectron.*, 2012, **36**, 18.
24 T. Sen, K. K. Haldar and A. Patra, *J. Phys. Chem. C*, 2008, **112**, 17945.
25 Z. Luo, X. Yuan, Y. Yu, Q. Zhang, D. T. Leong, J. Y. Lee and J. Xie, *J. Am. Chem. Soc.*, 2012, **134**, 16662.
26 S. Liu, J. Tian, L. Wang and X. Sun, *Sens. Actuators, B*, 2012, **165**, 44.
27 Z. Gao, M. Xu, L. Hou, G. Chen and D. Tang, *Anal. Chim. Acta*, 2013, **776**, 79.
28 Y. Jv, B. Li and R. Cao, *Chem. Commun.*, 2010, **46**, 8017.
29 J. Xie, Y. Zeng and J. Y. Ying, *Chem. Commun.*, 2010, **46**, 961.
30 Y. H. Lin and W. L. Tseng, *Anal. Chem.*, 2010, **82**, 9194.
31 Y. Jv, B. X. Li and R. Cao, *Chem. Commun.*, 2010, **46**, 8017.
32 F. Gao, Q. Q. Ye, P. Cui and L. Zhang, *J. Agric. Food Chem.*, 2012, **60**, 4550.
33 K. T. Carlson, G. W. Carlson and L. Tolbert, *Diabetic Med.*, 2013, **30**, 123.
34 S. Bellary, H. Cameron, K. Macleod, M. Malecha, K. Koria, P. Raja, J. D. Cabezudo and J. Ellison, *Diabetes Res. Clin. Pract.*, 2012, **98**, 430.
35 L. Yuan, W. Lin, K. Zheng and S. Zhu, *Acc. Chem. Res.*, 2013, **46**, 1462.
36 M. D. Allen and J. Zhang, *Angew. Chem., Int. Ed.*, 2008, **47**, 500.
37 P. Zhang, S. Rogelj, K. Nguyen and D. Wheeler, *J. Am. Chem. Soc.*, 2006, **128**, 12410.
38 H. S. S. Ramakrishna Matte, K. S. Subrahmanyam, K. Venkata Rao, S. J. George and C. N. R. Rao, *Chem. Phys. Lett.*, 2011, **506**, 260.
39 K. E. Sapsford, L. Berti and I. L. Medintz, *Angew. Chem., Int. Ed.*, 2006, **45**, 4562.